Thermochimica Acta, 160 (1990) 113–124
Elsevier Science Publishers B.V., Amsterdam — Printed in The Netherlands

FORMATION OF ORDERED STRUCTURES DURING POLYMERIZATION

I.LAMPRECHT, B.SCHAARSCHMIDT

Freie Universität Berlin, Institut für Biophysik,
D-1000 Berlin 33, Thielallee 63

SUMMARY

We report about the polymerization of polyacrylamide in open and covered petri dishes and the correlated appearance of polygonal structures. These structures transform from a "dissipative" type driven by the energy flow as consequence of polymerization heat production to "conservative" or static ones when they are "frozen in" by polymerization. The energetics of the process is investigated by means of calorimetry and thermography and compared with results of viscosimetry. The heat production by polymerization - determined calorimetrically to $\Delta H = -(90 \pm 5)$ kJ/mol acrylamid or 272 J/ml - and/or the evaporation of water at the surface are responsible for an adverse temperature gradient and the formation of these structures. The results are discussed with respect to the Ray-leigh- and the Marangoni-numbers of the polymerizing liquid and to possible mechanisms underlying this phenomenon.

INTRODUCTION

Ordered structures, periodic in time or in space, accompany our life and provoke admiration and astonishment. They bothered the scientists for many decades because they seemed to contradict the Second Law of Thermodynamics which states an ever increasing entropy and a decline of order. Nowadays it is clear that these structures appear in thermodynamically open systems far away from equilibrium, closed exporting more entropy to their surrounding than produced inside the system at the cost of the dissipation of energy. For this reason Prigogine [1] called such structures "dissipative".

On the other hand the degree of order of a physical system may be increased by an equilibrium process as cooling down as during crystallization or magnetization. The resulting structures, called "conservative", are static and have an infinite life time, because the system occupies one of its possible minima of potential energy. In contrast, dissipative structures are bound to a continuous flow of free energy through the system [2]. Coupling of different thermodynamic flows in an open

0040-6031/90/$03.50

system can produce "negentropy" and an organization of the system, if the overall entropy production of system + surrounding is positive. Systems with a dynamic organization are often taken as models for biological structures and living organisms [3].

One of the most intensively studied spatial structures is the hexagonal pattern formed in liquids when heated from below. They were first investigated by Benard [4] and explained by Rayleigh [5] in terms of conductive heat transport.

THEORETICAL BACKGROUND

Convection in a fluid layer sufficiently thin compared with the lateral extension is connected with mass and energy transport as a result of an adverse temperature or concentration gradient in vertical direction. The term "adverse" indicates that the system is potentially unstable. Both gradients can activate the "buoyancy engine" and/or the "surface tension engine" by causing the density of the liquid near the top to become greater than that near the bottom or by inbalances of surface tension forces [6,7].

In the first case, which is called a Rayleigh-Benard or thermal convection [because of the equation of state $\rho = \rho_0 (1 - \alpha T)$], a convective motion sets in if the ratio between the two competing forces, the buoyancy due to gravity and the friction due to viscosity, exceeds a critical value. This ratio, called the Rayleigh number, is given by

$$R_a = g \cdot \alpha \cdot \Delta T \cdot d^3 / (\kappa \cdot \nu) \qquad (1)$$

(with g standard acceleration of free fall, α cubic expansion coefficient, T absolute temperature and d height of the liquid layer, κ thermometric conductivity and ν kinematic viscosity). The critical Rayleigh number for water amounts to 658 for a surface open to air and to 1706 for a closed one [8].

In the second case, called Marangoni convection because of

$$\sigma = \sigma_0 + \delta\sigma/\delta T \cdot \Delta T + \delta\sigma/\delta c \cdot \Delta c \qquad (2)$$

(with σ surface tension, c concentration of solved substances) the two competing forces are the surface tension force and the viscous traction of the underlying fluid. A convective motion

sets in if the ratio between these two forces, the Marangoni number M_a,

$$M_a = - d\sigma/dT \cdot \Delta T \cdot d / (\rho \cdot \kappa \cdot \nu)$$
$$= - d\sigma/dT \cdot \Delta T \cdot d / (\eta \cdot \kappa) \qquad (3)$$

(with η viscosity) exceeds a critical value, which is reported in literature to be about 4000 [8]. Besides the external parameters (temperature difference, layer thickness) in both cases material parameters (viscosity, thermal conductivity) of the fluid determine the critical numbers for the onset of the convective flow. But both forces are capable of damping and destroying small mechanical and thermal disturbances in the preconvective period.

For most liquids at room temperature the surface tension forces are more effective than the buoyancy forces if the thickness of the fluid is less than 1 cm [9]. The surface tension is responsible for a concave free liquid surface above centers of ascending warm liquid, whereas the buoyancy must lead to a convex surface in these places [10,11]. In the usual case evaporation from a free surface favours both, buoyancy and surface tension mechanisms. The two mechanisms reinforce one another, are tightly coupled and yield the same cell pattern and cell size. Different species of cells can appear depending among other conditions on the viscosity of the liquid and the thickness of the layer [8].

In the following paper experiments of the formation of cellular pattern during the polymerization of polyacrylamide gel stained by methylene blue are presented. The aim was to calculate the horizontal and vertical temperature gradients during the exothermic polymerization process within a petri dish and to point out the underlying convective forces leading to an ordered spatial cell pattern. The results show an interesting transition from a dissipative to a conservative structure by "freezing in" the ordered motion of the liquid.

METHODS AND MATERIAL

Polymerization: The following recipe proved to give reproducible results at room temperature (20 - 30 ^{o}C).

Solution A: 0.1 % ammonium persulfate; B: 1 % N,N,N',N'-tetramethylethylenediamine (TEMED); C: 28 % acrylic acid amide (AA) and 0.75 % N,N'-methylene-bis-acrylamide (BIS); D:

concentrated methylene blue solution, all in bidistilled water. These four solutions were mixed in the following quota: 4A + 3B + 10C + 1D. Methylene blue is used to make the structure visible in transmis-sion light.

The mixture is poured into petri dishes (diameter 8 - 10 cm) in amounts rendering layers of 1 - 5 mm. The petri dishes remain open or are covered for a period of approximately 15 min during which polymerization proceeds and visible structures are manifested. After this time the supernating water layer above the gel is decanted and the dish is kept open for complete drying. The petri dishes used in these experiments were made from glass (bottom 2 mm thick, thermal conductivity 0.58 W/m·K) or polystyrol (bottom 0.75 mm thick, thermal conductivity 0.08 W/m·K). During structure formation the dishes rested on a 1-cm-thick layer of styropore (thermal conductivity 0.038 W/m·K).

Calorimetry: Heat production during polymerization was determined separately by means of a Calvet microcalorimeter with a working volume of 10 ml. Three components of the recipe were pipetted into the vessel, whereas the fourth component - either AA or TEMED - was kept in a glass spiral just above the vessel. After thermal equilibration the reaction could be started by pressing the solution in the spiral into the calorimetric vessel. The content of the vessel was continuously mixed by means of a mechanical stirrer agitated in a vertical direction by an electromagnet outside the calorimeter. After a few minutes the stirrer had to be stopped because of the increasing viscosity. Further details of the calorimetric method are described elsewhere [12]. The calorimeter renders a power-time-curve (heat production rate versus time) of the polymerization process, including the prepolymerization period, the maximum rate of heat production and the total heat evolved. Due to the thermal inertia of the instrument the output signal is "smeared" and has to be time corrected by the Tian equation [13] or by Fast Fourier Transform [14].

Thermography: Temperature distributions over the surface of the petri dishes during the polymerization reaction were measured by a thermography system (Philips/Hamburg) with an InSb-detector cooled with liquid nitrogen. The thermal resolution is quoted to

be 0.08 °C, the geometrical resolution to be 0.002 rad. During the experiments both resolutions figured to 0.2 °C and 2 mm at a temperature range of 2 °C. Temperature differences across the surface could be shown in 10 colours or 16 grey levels. Data were stored on video tape or directly photographed from the screen.
Cell size: The cell pattern, i.e. the cell size, the distance between adjacent cells and the height of the cell centers and cell boundaries, were determined optically, either by measurements of the structures in enlarged photos of the petri dishes or by direct inspection by means of a stereomicroscope with micrometer eye-piece. The ribs between two neighbouring cells could be even de-termined easily by means of a mechanical position transducer.

RESULTS

Heat production of polymerization

Fig. 1 shows a power-time curve of the polymerization reaction at 20 °C with the standard recipe. The solid curve represents the direct calorimetric signal and the dotted curve the time

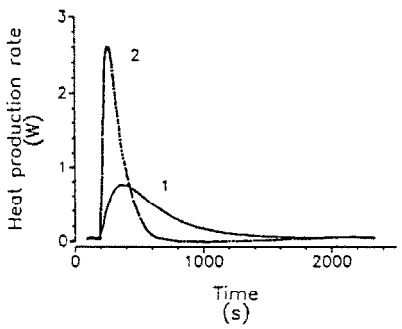

Fig. 1. Power-time-curve of the polymerization reaction of poly acrylamide gel at 30 °C. Line (1) represents the direct calorimetric signal, line (2) the heat production rate after time correction.

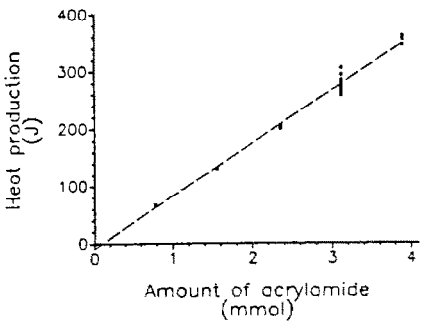

Fig. 2. Total heat production during polyrimerization of acrylamide (AA) as a function of the amount of AA.

corrected heat production rate corresponding to the "true" time scale. The pre-period of approximately 2 min known from the experiments in petri dishes is followed by a sudden increase in the heat production rate for about half a minute and a subsequent steady decline to the initial base line. The heat production ceases after about 15 min in good agreement with the visible structure formation in the petri dishes and no further increase in viscosity. From the area under the p-t-curve a total heat production of 272 J/(ml of final mixture) is determined which transforms to an enthalpy change of $\Delta H = -(90 \pm 5)$ kJ/mol AA (Fig. 2) close to the literature value of - 83 kJ/mol [15,16]. Though the recipe uses a small amount of the crosslinking monomer BIS as a copolymerisate the reaction is a first-order process as can be seen in Fig. 3 with an induction period of 17 s and a rate constant of 9.5×10^{-3} s^{-1}. A similar slope with corresponding values is found in a viscosimetric monitoring of the polymerization. As TEMED is present in minor amounts (1% in weight of AA in the final mixture) its polymerization heat does not contribute significantly to the total heat output.

It is known from the literature [16] that the heat production during the first addition of monomers is very high and that it decreases during the further additions. Moreover, increasing viscosity of the solution slows down the rate of reaction and makes it limited by diffusion processes. Such a time course is in good agreement with the time corrected calorimetric curve in Fig.1.

Temperature distribution

Fig. 4 presents the temperature distribution on the upper surface of a petri dish. It was derived from the video screen of the infrared camera and shows the momentary temperature after 10 min as spots in a specific distance from the base line. The maximum deviation amounts to 2 °C. It becomes clear from the graph that there is a steep temperature gradient directly at the periphery of the polymer and a more or less homogeneous distribution throughout the dish. In a sequence of video pictures one can easily follow the establishment of the temperature gradient and of some annular temperature structures changing with time. But with resolutions of 0.2 °C and 2 mm it is not possible to determine clear hexagonal structures by eye.

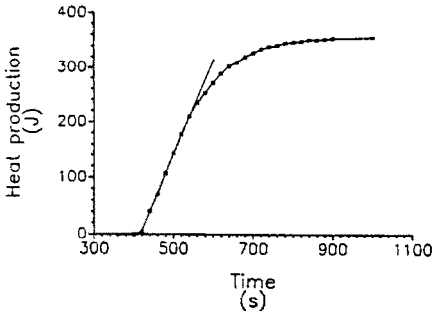

Fig. 3. Time course of the total heat production during polymerization. The straight line indicates the period of the first order reaction.

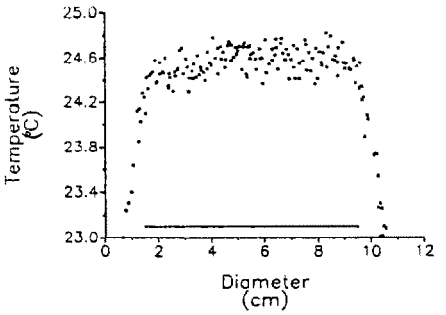

Fig. 4. Temperature distribution over the upper surface along a diameter of a petri dish 10 min after staring the polymerization reaction. The bar indicates the position of the petri dish (inside edge).

Thus we can conclude that the maximum temperature difference in the radial direction as well as in the vertical direction is 2 °C which occurs approximately 10 min after starting the reaction. This difference can be used as an upper limit for the estimation of the heat transfer through the fluid layer within a petri dish.

Heat balance

The layer of the polymerizing liquid in the petri dishes amounts to 1 to 5 mm. From the calorimetric data of 272 J/(ml of final mixture) one obtains 27 to 136 J/(cm^2 of surface) over a time of 15 min (Figs. 1 and 2) which equals a power of 30 to 150 mW/cm^2. In a completely adiabatic case the produced heat would rise the temperature in the layer between 6.5 and 32.5 ^{o}C, respectively. Obviously, the heat of polymerization is the only heat source in the system. On the other hand there are two heat sinks in the system: a heat loss due to evaporation of water at the top surface in the open petri dishes and a heat flux through the boundaries of the petri dish - the lateral rim, the bottom of the dish and the surface of the covered dishes. Since the ratio of the lateral extension to the thickness of the fluid layer within a dish is about 1:100 we can neglect the lateral heat

losses. The losses by heat conduction through the material forming the boundary can be calculated from the equation of heat conduction. With the known values of the thermal conduction resistance in glass, polystyrol and styropore (3.45×10^{-2}, 9.26×10^{-2} and 26.16×10^{-2} $m^2 \cdot K/W$, resp.) one obtains a heat flow of 0.67 $mW/(cm^2$ of bottom surface) for the glass dish and 0.56 mW/cm^2 for a polystyrol dish. When the dishes are covered the corresponding figures amount to 5.8 and 2.2 $mW/(cm^2$ of rim or cover surface), resp. These figures demonstrate that in covered petri dishes heat passes mainly through the upper surface.

During the polymerization period in petri dishes the weight of the complete arrangement (dish plus mixture) was followed continuously and yielded a loss of 556 mg/h or 8.74 $mg/(h \cdot cm^2$ of surface). Assuming that the total loss corresponds only to evaporation of water (evaporation heat 40.7 kJ/mol) a power of 5.97 $mW/(cm^2$ of surface) is required. In open dishes with evaporation the heat loss from the upper surface is thus tenfold higher than the flow through the bottom establishing the adverse temperature gradient mentioned above.

Structure Formation

Approximately 5 min after starting the reaction the first blue lines in the liquid layer appear and proceed to form more or less ordered structures which are manifested after another 10 min due to the solidification of the gel. Ordered structures were obtained at room temperature (20 to 30 ^{o}C) in petri dishes resting on a styropore plate and with fluid layers between 1 mm and 5 mm thickness. The occurrence of structures were independent of the material of the petri dish and whether the dish was covered or open to air. Cell structures could scarcely or not at all be observed if the ambient temperature exceeded 40 ^{o}C or if the dishes rested on a metal plate and/or were heated from below. Polymerization in metal dishes on metal plates never showed any structuring as the heat flow through the bottom exceeded that at the surface due to the high thermal conductivity of the material.

Fig. 5 shows examples of cell pattern with different types of cells. In general irregular polygons (number of sides between 4 and 7) up to 3 mm in diameter, ribs, streamers and vermiculated rolls with length of several centimeters were observed (Figs. 5a,c). In some cases even superstructures occurred in form of a

hexagon with centre or (Fig. 5b) or further structures within the polygon. The cell pattern itself could not be attributed to certain experimental conditions. Only in cases of predominant polygonal structures (Figs. 5c,6a) the size of the cells (radius of a circle of equivalent area) depended on the height of the liquid layer (Fig. 6b). This graph was obtained by measuring the cell dimensions of 150 cells in different patterns. It could be observed directly by eye and by microscope during the reaction, that the boundaries of the cells corresponded to ascending coloured flows. Needleshaped crystals of methylene

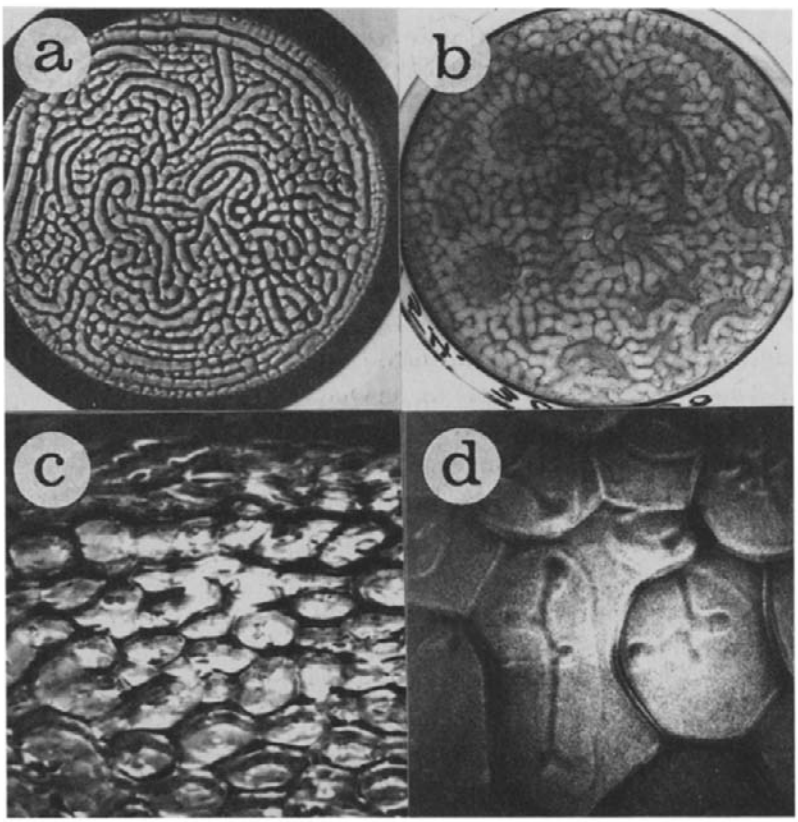

Fig. 5. Different typical cell pattern formed during polymerization: a - total view of a petri dish with polygons and vermiculated rolls; b - with a centered hexagonal superstructure; c - view to the polymer surface under a flat angle showing the upright standing walls between the cells; d - additional structures within the polygons.

blue oriented their longer axis parallel to the liquid flow, horizontally to the ribs, vertical within the ribs and starlike to the corners of adjacent polygons. After solidification of the gel the centers of the cells were found to lie below the cell boundaries so that the cells appeared as been surrounded by walls. These differences in surface elevation were about 3 - 5 μm directly after solidification. When the gels were completely dried the elevation of knots and ribs amount to more than 500 and 300 μm, resp.

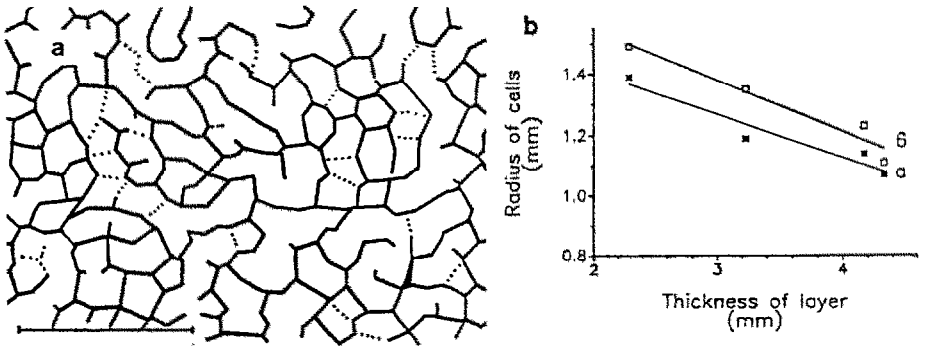

Fig. 6. Polygonal cell structure. (a) Enlarged drawing of a polygonal cell structure. (b) Cell radius of polygons as a function of the height of the fluid layer.

The dried gels could be removed from the petri dish (carefully! because the resulting gel occupies less volume than the original monomer mixture and disrupts) by bending the bottom of the plastic dish and withdrawing it by a spatula. The structures were conserved even if the gel was completely dry and solid. For instance, Fig. 5a was taken several years after the corresponding experiment.

Rayleigh- and Marangoni-number

Since the final mixture of the polymerizing fluid (compare recipe above) contains more than 79 % of water the dimensionless Rayleigh- and Marangoni-numbers, R_a and M_a, can be estimated. Their values determine whether the system under investigation will become unstable or not. With the numerical values for water

at 20 °C (mass density 0.998×10^{3} kg·m^{-3}, cubic expansion coefficient 1.8×10^{-4} K^{-1}, thermometric conductivity 1.43×10^{-7} m^{2}·s^{-1}, kinematic viscosity 1.01×10^{-6} m^{2}·s^{-1}, viscosity 0.998×10^{-3} J·s·m^{-3}, standard acceleration of free fall 9.81 m·s^{-2} and thermal gradient of surface tension 1.5×10^{-4} J·m^{-2}·K^{-1}) the following expressions are derived

$$R_a = 12.3 \cdot \Delta T \cdot d^3 , \tag{4}$$

$$M_a = 1.05 \times 10^{3} \cdot \Delta T \cdot d , \tag{5}$$

with the temperature difference ΔT in K and the layer thickness d in mm. Taking into account the maximum measured temperature gradient of 2 °C and layer thicknesses of 1 to 5 mm, R_a calculates from 25 to 3075 and M_a from 2100 to 10500. Comparing these values with the above mentioned ones of R_a = 658 for an open surface, 1706 for a closed one and M_a = 4000 it turnes out that both forces, buoyancy as well as surface tension, may account for the pattern formation.

CONCLUSION

Convective flows due to evaporation at the surface are widespread in nature; they appear in lakes, in bathtubs or in teacups, as the famous "wine tears" of J.Thompson, as cellular cloud pat-terns or sun spots. Usually, they are not seen in liquids by the naked eye, but brought to vision by means of schlieren methods or floating particles. They exist as long as a driving energy flow exists and vanishes with time. Here, we showed experiments to preserve the transient structures by polymerization, in the sense of "freezing them in". Similar results are sometimes seen in the drying coat of paint or during solidification of glass. The polygons shining up in the polymers are not as regular as those in Benard experiments as the time before final polymerization is too short to establish a stable convective flow necessary for the appearance of regular structures. Nevertheless, all forms known from liquid dissipative structures are found, conservated for long times in the polymers.

ACKNOWLEDGMENT

U.Wendker observed the structures for the first time in 1975 and developed the initial recipe. In the following years C.Schu-

ster and G.Welge helped with the experiments. J.Glandien performed the thermography and taped the pictures. To all of them we are deeply indebted.

REFERENCES

1 I. Prigogine and G. Nicolis, On symmetry-breaking instabilities in dissipative systems, J.Chem.Phys. 46 (1967) 3542- 3549

2 I. Lamprecht, Review of the Theory of Dissipative Structures, in: I. Lamprecht and A.I.Zotin (eds.), Thermodynamics of Biological Processes, de Gruyter, Berlin, 1978, pp.261-276.

3 G. Jetschke, Prinzipien der spontanen Strukturbildung in Physik, Chemie und Biologie, Biol.Rdsch. 21 (1983) 73-92.

4 H. Benard, Les tourbillons cellulair dans nappe liquide transportant de la chaleur par convections en regime permanent, Rev.Gen.Sci.Pures Appl.Bull.Assoc. 11 (1900) 1261-1271 and 1309-1328.

5 Lord Rayleigh, On convection currents in a horizontal layer of fluid, when the higher temperature is on the under side, Phil.Mag. and J.Sci. 32 (1916) 529-546.

6 S. Chandrasekhar, Hydrodynamic and Hydromagnetic Stability, Oxford University Press, London New York 1962.

7 C. Normand, Y. Pomeau and M.G. Velard, Convective instability: A physicist's approach, Rev.Mod.Phys. 49 (1977) 581-642.

8 J.C. Berg, A. Acrivos and M. Boudart, Evaporative convec tion, Adv.Chem.Eng. 6 (1966) 61-123.

9 J.R.A. Pearson, On convective cells induced by surface tension, Fluid.Mech. 4 (1958) 489-500.

10 H. Jeffreys, The surface elevation in cellular convection, Quart.J.Mech.Appl.Math. 4 (1951) 283-288.

11 L.E. Scriven and C.V. Sternling, On cellular convection driven by surface tension gradients, J.Fluid.Mech. 19 (1964) 321-340.

12 A. Anders, G. Welge, B. Schaarschmidt, I. Lamprecht and H. Schaefer, Calorimetric investigations of metabolic regulation in human skin, in: I. Lamprecht and B. Schaarschmidt (Eds.), Applications of Calorimetry in Life Sciences, de Gruyter, Berlin, 1977, pp.199-208

13 W. Hemminger and G. Höhne, Calorimetry. Fundamentals and Practise. Verlag Chemie, Weinheim 1984.

14 K.H. Müller and Th. Plesser, Deconvolution of periodic calorimetric data by Fast Fourier Transform, Thermochim. Acta 119 (1987) 189-201.

15 C.J.O.R. Morris and P. Morris, Physico-chemical measurements in polyacrylamide gels, in: Electrophoresis and Isoelectric Focusing in Polyacrylamide Gel (R.C. Allen and H.R. Maurer, eds.), W. de Gruyter, Berlin 1974, p.9-15.

16 F.S. Dainton and K.J. Ivin, Heats of polymerization, in: H.A. Skinner (Ed.), Experimental Thermochemistry, vol.II, Interscience Publisher, New York, London 1962, pp.251-280.